International Journal of Scientific Research and Engineering Development-– Volume3 Issue 1, Jan-Feb 2020

Available at www.ijsred.com

RESEARCH ARTICLE OPEN ACCESS

3D Seismic Structural Interpretation of Riche Field, Onshore Niger Delta

Abimbola.L. Abiola[1]; Emujakporue Godwin[2]

[1]*Department of Petroleum Geosciences, Centre for Petroleum Geosciences, Institute of Petroleum Studies, University of Port Harcourt, Nigeria*

(bimbolah.abiola@gmail.com)

[2]*Department of Petroleum Geosciences, Centre for Petroleum Geosciences, Institute of Petroleum Studies, University of Port Harcourt, Nigeria*

(godwin.emujakporue@uniport.edu.ng)

----------**********----------

Abstract:

3D seismic reflection data integrated with well logs data were employed in this study to recognize the structural features and evaluate the hydrocarbon trapping mechanism of Riche field, Onshore Niger Delta. Well to well litho-stratigraphic correlation was conducted on the four (4) Riche wells to detect the sand units containing hydrocarbons. Two hydrocarbon-bearing reservoirs were depicted and their lateral continuity was established using the gamma-ray, Deep resistivity, Neutron, Density and Sonic logs. Checkshot data made available for Riche well2, together with sonic and density logs were used to compute a synthetic seismogram and carry out seismic to well tie which specified the position of the reservoir of interest on seismic. Seismic volume attributes functioned in the manual and auto tracking mapping of faults and seventeen (17) faults were manually interpreted across the field. The horizon for the reservoir of interest was picked on the inlines and crosslines of the seismic volume to produce structural maps in time and depth. The time and depth structural maps showed a four-way closure minor faults assisted structure. This technical effort provides a basis to develop a reservoir model and estimate of the volume of the hydrocarbon accumulation.

Keywords **—Structures, Trapping, Hydrocarbon, Faults,Synthetic Seismogram**

----------**********----------

I. INTRODUCTION

Over the years, the search for hydrocarbon has not been limited to where they were before (surface supplies), but also where conditions which renders it possible for the entrapment and storage of hydrocarbon generated from the mature source rock are exhibited. The components and processes vital for hydrocarbon occurrence and accumulation are termed the petroleum system and it defines the foundation for developing and producing from a field. In concordance with (Oilfield Review Summary, 2011), the essential elements; Kerogen-rich source rocks, reservoir rocks, trap, seal and overburden rocks, must be stationed for the occurrence and accumulation of hydrocarbons while the processes are the conditions that take into consideration petroleum accumulation (Henriksen et al, 2011). Structural interpretation helps to properly locate wells which could be exploration wells, field development wells, field production wells, to discover new reserves, and to efficiently produce discovered reserves. Also, structural analysis helps in delineating the size of hydrocarbon reserves (how many barrels), to determine trap integrity (how good is the trap, is the fault through the reservoir zone sealing or non-sealing), to understand basic

architecture which is a helpful in predicting source maturation and also for modelling hydrocarbon migration (Bjørlykke, 2010). 3D Seismic interpretation is done to image the earth's subsurface structure to offer a proper understanding of its spatial and temporal evolution. It is furthermore done to trace stratigraphic and structural features that may contain exploitable hydrocarbon resources (Christopher, 2012).Seismic structural interpretation which is the focal point of this work can be applied in the interpretation of structures to detect discontinuities, folds, uplifts and other structural elements. Structural settings such as extensional basins, strike-slip basins and interpret structural styles can be interpreted. Seismic ensures 3D consistency in structural interpretation. Seismic structural interpretation ascertains timing relationships particularly when the traps formed in relation to when hydrocarbon was generated and migrating (Lowell, 1985).The principal aim of this work is to access the subsurface structures available for possible accumulation of trapped hydrocarbon. The thesis focuses mainly on building a structural framework derived by faults mapping and horizon interpretation of continuous events using manual and automatic method, to generate structural maps. This is attained through well-to-well correlation of sand units. The sub-surface geological structural map generated is the basic deliverables of a seismic interpretation can either be depth (depth-converted seismic data) or two-way travel time structure in time-migrated data. This 3D visualization is useful in presenting the product of seismic interpretation in an easy-to-understand form. These structural maps represent 3D shape of the mapped horizons within Riche field to spot fault structures and closures which the fault offsets form around the hydrocarbon bearing zones. This study is put into operation using the Schlumberger Petrel software.

The study area 'Riche Field' is located onshore Niger Delta and the coastal swamp depobelt. In subject to the Niger Delta, its development commenced during the late Palaeocene/Eocene when sediments begun to build out over trough between basement host block of northern flank of the today delta area (Turtle et al, 1999). Akata, Agbada and Benin occur in the depobelts and they are defined by the syn-depositional faulting system (growth faults), roll over anticlines and low structures resulting from rapid deposition, seaward progradation and differential compaction of sediment (Selley and Morril 1983).

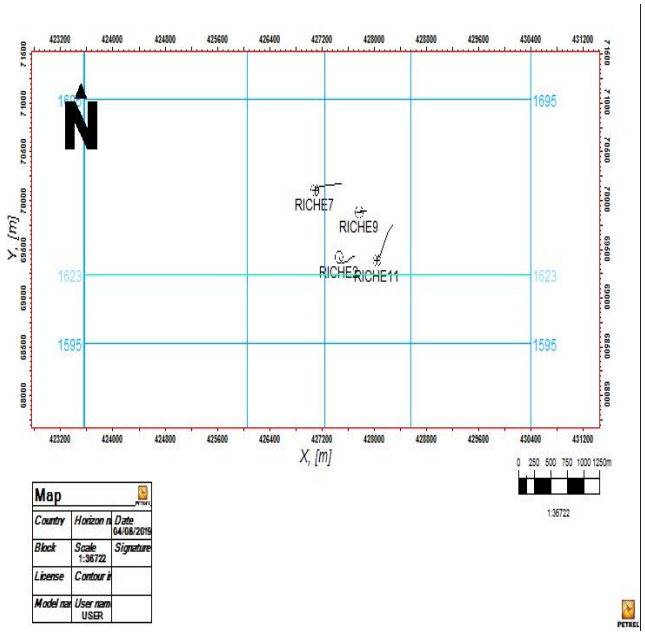

Figure 1: Base map the distribution of the four wells across Riche field

II. MATERIALS AND METHODS

The work procedures for this work include data assessment, project setup, data loading, well correlation and reservoir delineation, volume attributes and faults mapping, well to seismic tie, horizon mapping, time surface map generation and time-depth conversion. Dataset inventory was implemented to be sure of the reliability of the data to be used for the project. The well header and well logs were examined for possible discrepancy and challenges. Availability and effectiveness of the logs such as density and sonic for the seismic-well tie processed undertaken was ensured. The source of velocity (Checkshot) was also verified to ensure authenticity. Adjustments were made on the well

header information, well names and unique well identifier (UWI) which were mismatched and not properly spelled were corrected using the Microsoft excel tool.

Nature/Sources of Data

The data available and used for this study was provided by Shell Petroleum Development Company. The data set include; 3D seismic volume with 274 numbers of inlines and 256 numbers of crosslines. The inlines are found between 5575m to 5850m and the crosslines range is from 1495m to 1750m. The seismic was shot at an interval of 4ms. The magnitude of samples per trace was 301 samples, inlines and crosslines interval was 25m as it appears in the survey geometry information. Well header data for Riche well 2, 7, 9, and 11, well deviations or directional survey data for the four wells, well logs (GR, Deep resistivity, Neutron, Density and Sonic Logs) for four wells and checkshot data for Riche 2 well. The well logs, well logs header and deviation data were all provided in digital ASCII format.

Data Importation

All data used were entered from the dataset folder in the drive C of the work station used into Petrel 2015 software. Each data has its supported file type that allows the data to be imported into the interface. The petrel's window input pane is a link to the dataset folder and houses the all data imported for the project purpose. The 3D seismic data provided is a 960km^2 field and was introduced from the dataset folder using *SEG-Y Seismic data (*.*)* file type format into the input pane of the petrel interface. The seismic data was imported as seismic default template with elevation time as its domain. The well header houses the well name, UWI, surface x, surface y, well datum and total depth (md) information for Riche 2, Riche 7, Riche 9, and Riche 11. The header was inserted using the *well heads* (*. *) into the interface. The well deviations for Riche 2, 7, 9 and 11, which contains measured depth (MD), inclination and Azimuth information were inserted into the wells using the *Well path/deviation for surveys (ASCII) (*. *)*. The project units for the logs are specified in depth. The file format for import of well logs for the four wells is well logs (ASCII) (*. *). To import the checkshot data into petrel, checkshot format (ASCII) (*. *) file format was used. It was ensured that the checkshot was connected to well that has the checkshot, which is Riche well 2. The number of header lines used was 1. The checkshot data contain the two-way travel time (TWT) with measured depth information.

Well Correlation and Reservoir Delineation

Magnitudes of a particular formation property are usually measured by logging tools put into effect by a logging truck which lowers the downhole instruments into the wellbore (Schlumberger, 2009). The logging data derived from logging are used to correlate zones across wells and support in hydrocarbon evaluation such as structures and isopach mapping, determine depths, determine depths and thicknesses of hydrocarbon bearing zones, distinguish between hydrocarbon fluids in reservoir and evaluate hydrocarbon reserves of the zones of interest.The four wells and required logs (GR, deep resistivity/ILD, neutron/NPHI, density/RHOB and sonic logs) were displayed side by side on the well section window in the petrel interface. The scales of each log were set. The GR log is commonly the first log on the log tracks. Shale cut-off was determined on a bimodal plot and a minimum value of 0 and maximum value of 150 was used as a range for the GR logging records. The minimum value for the deep resistivity logs is 0.2 and a maximum value of 2000. The neutron and density were combined together on the third track by reversing the NPHI. The scale used for the density log is 1.65 and 2.65 for the minimum and maximum values respectively. The minimum value for the neutron log was 0 and 60 for the maximum value. The wells placement on the well section was arranged based on closest neighbors with the help of the information on the base map and cross section with Richie well 7 as the first, followed by wells 2, 9 and 11 as viewed in figure 2. The four wells were flattened on depth at 3200m. The sand bodies for all the

wells were picked and correlated starting from the deepest well with the GR log motifs and shale thickness. The reservoirs were determined using the deep resistivity, neutron-density and acoustic logs. The fluid type (water, oil or gas) in the sand unit were found out using the deep resistivity logs. The sand zones which contained oil were discriminated from those that contained gas with the neutron-density combined logs.

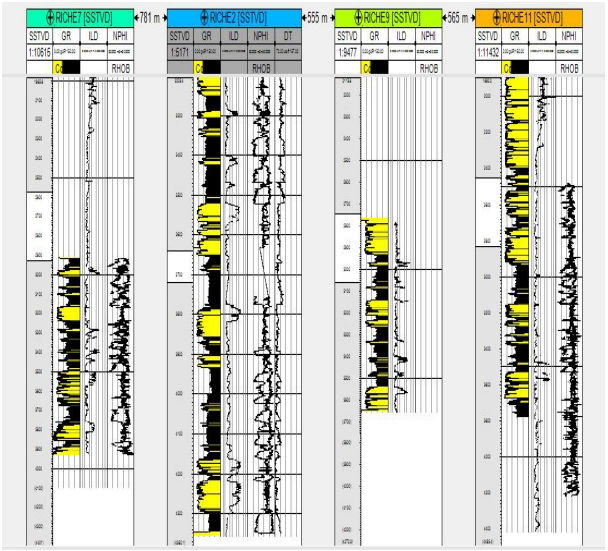

Figure 2: A well section showing the four (4) Riche well logs

Seismic to well tie Process

The process of seismic to well tie is a synthetic modelling process. It involved building an artificial seismic and comparing it with the actual seismic. To effectively perform well-seismic tie, certain logs are required; density log (gm/cm^3) and sonic logs (us/ft). From seismic, a wavelet is needed. The course of action for the standard well-seismic tie modelling, as demonstrated in the subsequent headings, started with giving the well a time function, then calibrating the sonic with the checkshot in the process called sonic calibration. The calibrated sonic now bears both checkshot and sonic information. After the sonic calibration, acoustic impedance log was created which served an input for the reflectivity coefficient log. The computation of the acoustic impedance and reflectivity coefficient was automatically effected by Petrel. This reflectivity log which is a log input was then converted to a seismic wave by convolving it with a wavelet from seismic. Analytical, statistical and deterministic wavelets were compared to determine the right size of the peaks and troughs. The Ricker wavelet was used and its frequency was adjusted to give the right model for the artificial seismic of the seismic-well tie process. The position of the synthetic seismogram was also adjusted by bulk shifting to give a good similarity with the actual seismic.

A.Assigning Time Function to the Well

After attaching and importing the checkshot to the Riche well 2, the elementary step is to assign the checkshot to the Riche well2 (in depth) to convert it to time. The checkshot which serves as velocity function links the seismic and the well and enables the well to be visible and placed on top of the seismic section. The time function is assigned to the Riche well 2 which has the checkshot information by running the checkshot on the well. This now assigns a two-way travel time function to the Riche well 2 which appears on the Riche well2 spread sheet. The Riche well 2, which is a point data, is seen on the seismic line that intercepted the well.

B. Creation of Well Intersection

After applying the time function to Riche 2, an intersection was created around Riche well2 vicinity using a horizontal plane extension of 1000 by 1000. The saved copy of the intersection was then converted to 2D seismic. This seismic as seen in figure 3 was employed for the well-seismic tie computing.

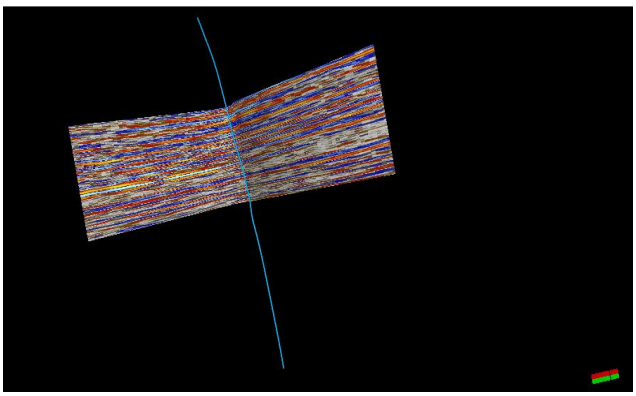

Figure 3: A well intersection around well 2

C.Sonic Calibration

This process is accomplished on the seismic to well tie toolbar of seismic interpretation in petrel. The sonic calibration was carried out on Riche 2 which contains the checkshot information by creating a new study for the process. The log inputs parameters were the sonic log and checkshot readings of Riche 2. The checkshot adjusts and calibrates the sonic log. The outputs from the sonic calibration are the calibrated sonic, TDR, integrated sonic, Knee points, knee curve and residual drift.

D. Synthetic Seismogram Generation

The generation of synthetic seismogram which is a forward modelling process is a seismic representation of the well and was made to derive a time-depth relationship in order to fit well events to seismic events in the seismic-well tie process (Simm and Bacon, 2014; Robein, 2003). The input parameters for the synthetic generation are the TDR from Riche2 checkshot, wavelet (zero-phase) and the Reflection coefficient. The Reflection coefficient method used was sonic velocity and density (Acoustic impedance). The histogram shows the distribution and frequency of the logs. The reflection coefficient was derived from the acoustic impedance calculation. The analytical, deterministic (extended white, Isis frequency, Isis time) and statistical (extraction and extraction extended) wavelets were tried out. A zero phase ricker wavelet of 22Hz was afterwards used for this artificial seismic generation process. Adjustments were made on the frequency of the ricker wavelet. Shrinking of the wavelet frequency reduced the amplitude of the seismic reflections. The output for the study is the seismogram, reflectivity and computed acoustic impedance. A bulk time shift of -22ms was applied to further align and correspond with the peaks and troughs on the seismic to that of artificial seismic in the well to well-seismic tie process. The synthetic seismogram shows a good similarity with the original Riche seismic.

Seismic Volume Attributes Realization and Faults Mapping

Several structural volume attributes were realized on the seismic volume to increase the continuity of the seismic reflections and reveal the faults structures better on the seismic lines. For the manual interpretation, discontinuity cubes were realized on the main seismic. The trace AGC attribute was initially realized on the Riche seismic. Then structural smoothing volume attribute was also realized on the actual volume of seismic and the variance attribute on the structural smoothing realized attribute. The structural smoothing variance attribute's horizontal or Z time slice was placed upon the 3D window while the inline of the structural smoothing attribute was viewed on the interpretation window. The variance attribute isolated the red and blue colors and darkens the discontinuities. The inline was a preferred direction to map the fault structure as it is a line perpendicular to the geologic strike and it revealed more structures. The inline showed the trend of the faults with depth. The time slice showed the lateral extent of the faults.

The tool used for the fault mapping on petrel is the seismic interpretation tool palette. The 3D window and the interpretation window were used to display the seismic lines on the petrel interface for the mapping of the discontinuities. The interpretation and 3D windows were laid out on a single vertical window so as to view them concurrently as the fault mapping is done. A fault with a clearer continuity was first mapped on the time slice on the 3D window to give a guide on where the faults start and terminates and establish the lateral extent. Dotted lines are seen on the inline on the intersection window. The dotted lines showed the interception of where the fault was mapped on the time slice. This serves as a guide to map the fault on the inline across the entire volume on the interpretation window. As the mapping was performed on the inline, the track of the plotting was seen on the time slice. This process was repeated for the other faults lines that were mapped. This work flow was exercised to map seventeen (17) faults on the seismic volume. The faults were mapped across the seismic volume of the survey area at interval of 10m.

After the manual interpretation of the faults, the ant tracking attribute volume was applied to automatically extract faults from fault attributes. The ant tracking attributes algorithm uses the principles of ant colony to extract these surfaces (Zhao and Sun, 2013). The ant track volume was realized on top of the original seismic, structural smoothing and structural smoothened (variance) pre-processed seismic volume. The parameter applied for the realizations was the aggressive ant mode.

Horizon Interpretation and Time structural Map Generation

After the seismic-well tie has been properly done to confirm where the reservoir top corresponded on the seismic and synthetic seismogram, a modified TDR is obtained owing to the adjustments made on the synthetic seismogram. The Diamond reservoir top across the four wells was chosen as the reservoir of interest to be mapped across the seismic. An amplitude gain correction was applied on the seismic volume to enhance the amplitude to aid in the mapping of the horizon. The horizons were mapped on the in-lines and cross-lines across the seismic cube.

An increment of 16 and then 8 was exercised for the inlines and crosslines mapping exercise. A seismic seed grid was derived after the manual interpretation of the horizon. From the seed grid created, fault lines were seen and seven (7) fault polygons were constructed around the faults. Polygon 6 served as the boundary around the structure and polygon 8 served as the fault center polygon. Around the grid, a boundary polygon was drawn. The contour interval used for the surface was 25ft and a time structural map was gotten from the horizon mapped. During the interpretation, the consistency of the horizons picked and the faults polygons were checked with the seismic data volume.

Time-Depth Conversion

The final step in the structural interpretation of the diamond reservoir involved the time-domain to depth-domain map conversion. The velocity function that served as a TDR to convert the time horizon interpreted to depth was the original checkshot velocity. A non-linear 3rd order polynomial function was utilized to make the plot of Twt against depth as observed below in figure 4.

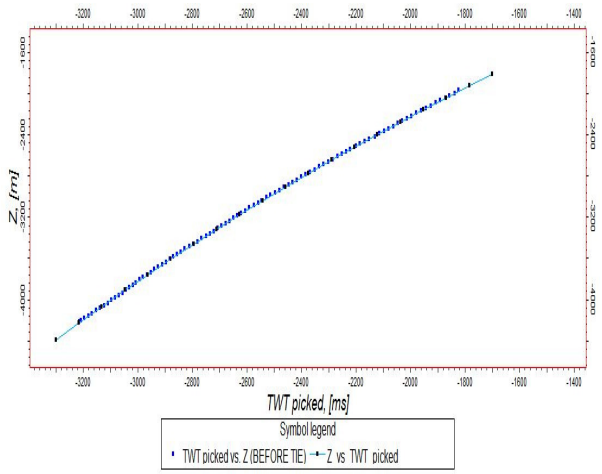

Figure 4: Riche checkshot plot (TWT vs. Depth)

III.RESULTS

The well logs correlated reveals two reservoir zones which are the Diamond and Gold reservoir tops at depths. Seventeen (17) faults were recognized and mapped on the inline and time slice of the seismic section. The synthetic and antithetic faults are listric in nature (Growth faults). The seismic to well tie showed that Riche well has a good peak to peak and trough to trough conformity. The mapped hydrocarbon reservoir surface intersects on the trough of the seismic section as observed from the seismic-well tie process and this corresponds to low impedance sand (Class3 AVO).

Result of Well to Well Correlations and Reservoir Identification

The Gamma radiation, Deep resistivity, Density, Sonic and Neutron logs were inputted to achieve the proper correlation from one well to the other and delineation of the reservoirs over the four wells drilled in

different locations of the Riche field. Riche 11 well was discovered to be the deepest (4460m) after flattening on depth across the four wells.

The differences in rock types (reservoirs and non-reservoirs) were distinguished using the shale cut off of 56gAPI unit which was obtained from the bimodal plot of the GR records. The high gamma-ray values showed the shale zones which the non-reservoir units while the low gamma-ray values were the sands which are the reservoirs. The tops of the sand bodies picked and correlated are viewable in figure 5.The high resistivity sand zones accommodate hydrocarbons. The balloon shape typified gas while the crossing of the two logs evinced the presence of oil in the reservoir as seen on neutron-density logs in figure 5. Two reservoirs zones were spotted named the Diamond and Gold reservoirs. The log-picked wells also showed the presence of faults between the sand units across the wells.

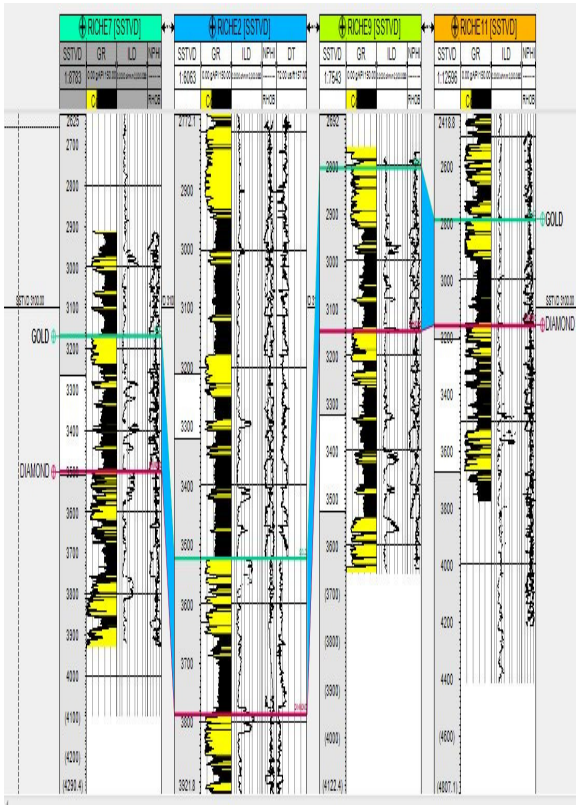

Figure 5: Cross-section of the Riche correlated reservoir tops

Result of Seismic to Well Tie

In the synthetic seismogram computing/seismic to well tie procedure, a time function was assigned to Riche well2 using its checkshot data. This checkshot plot of Twt against depth showed a steady trend of no outliers.After the time function was applied to the well, Riche well 2 appeared on the line where it intercepted the seismic as denoted in figure 6. The tops of the reservoirs were also posted on the seismic alongside the well. The inputs and output of the sonic calibration is sited on a well section window indicated in figure 7. The section shows the DT and RHOB logs, the resulting calibrated sonic log and the residual drift which is the difference between the original sonic log and the calibrated sonic log.

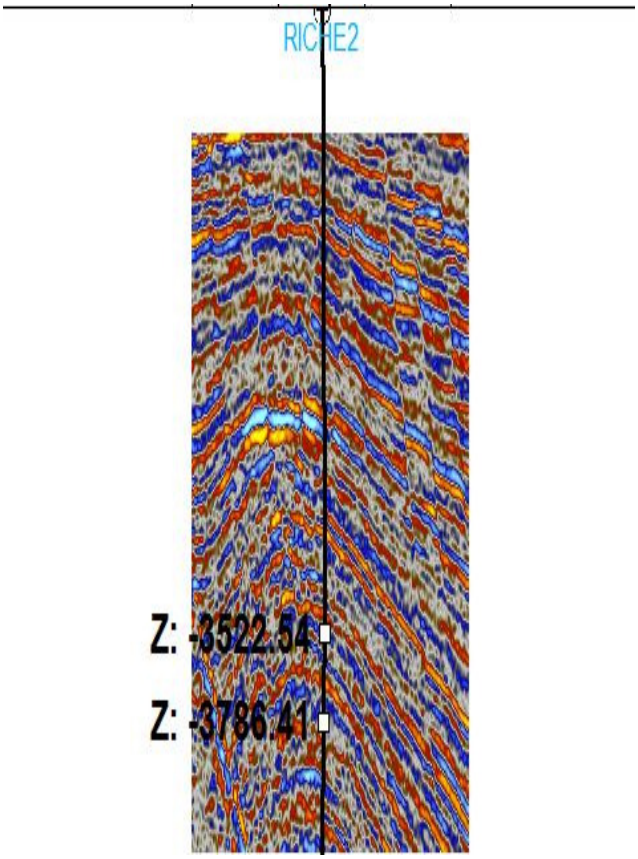

Figure 6: Seismic line through Riche 2 well

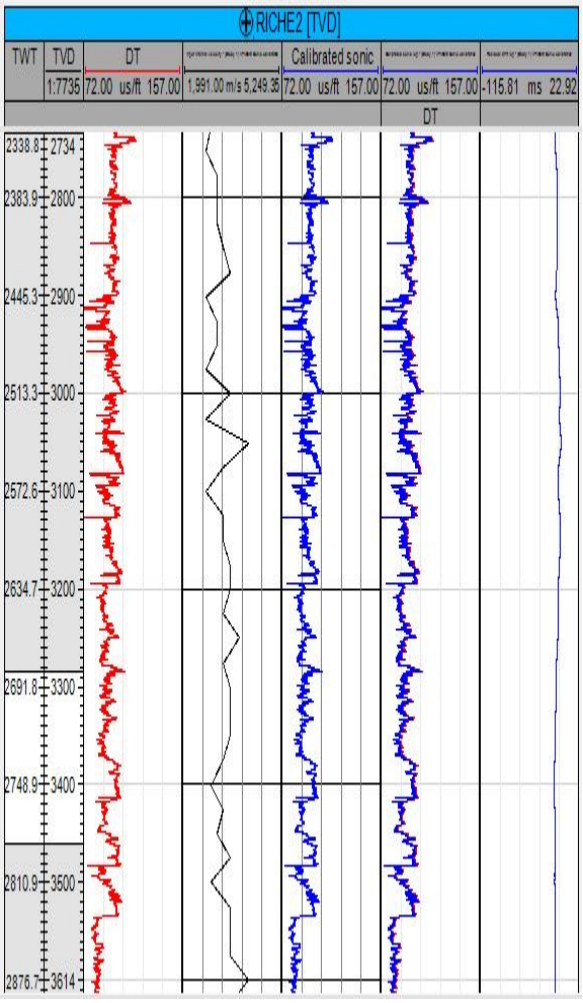

Figure 7: Calibrated sonic log plate

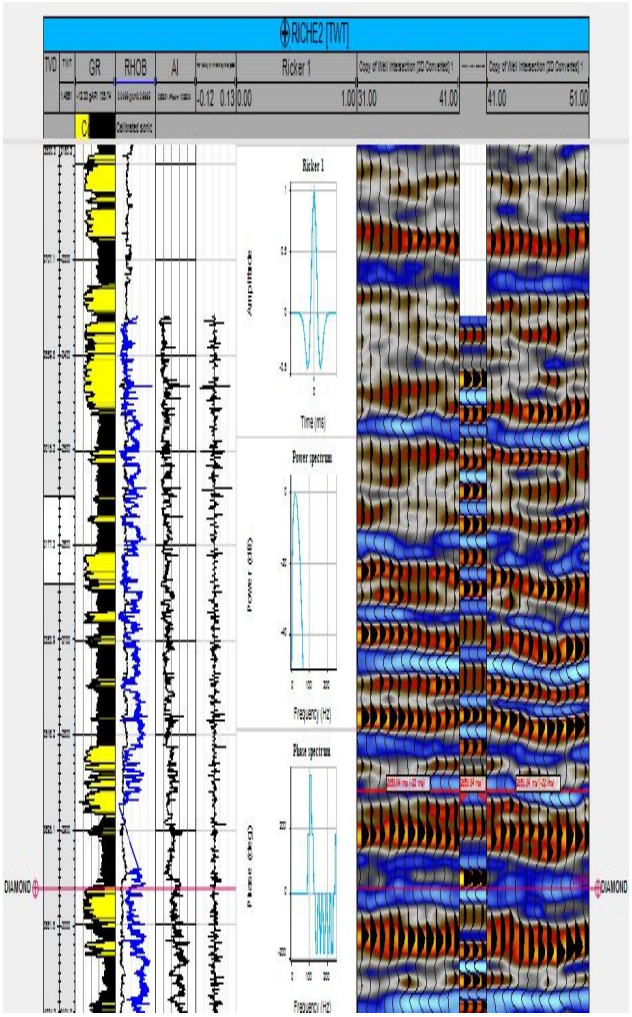

Figure 8: Riche 2 synthetic seismogram section

A 1D or well seismic known as the artificial seismic or synthetic seismogram was generated after convolving the reflectivity coefficient with the Ricker wavelet. The artificial seismic generated showed that the Riche well 2 have a good time-depth tie with a peak to peak and trough to trough match as seen on figure 8. From the well to seismic tie attained, the top of the Diamond hydrocarbon bearing sand unit lie on the trough event of the seismic section. Figure 8 shows the synthetic seismogram of Riche 2 and the mapped Diamond well top.

After the seismic to well tie was done, a new time depth relationship was generated as a result of the adjustment made on the artificial seismic. A graph of the original checkshot used prior to the seismic to well tie was plotted against the new TDR as revealed in figure 9. The outcome demonstrates there is no much difference between the two TDR plots.

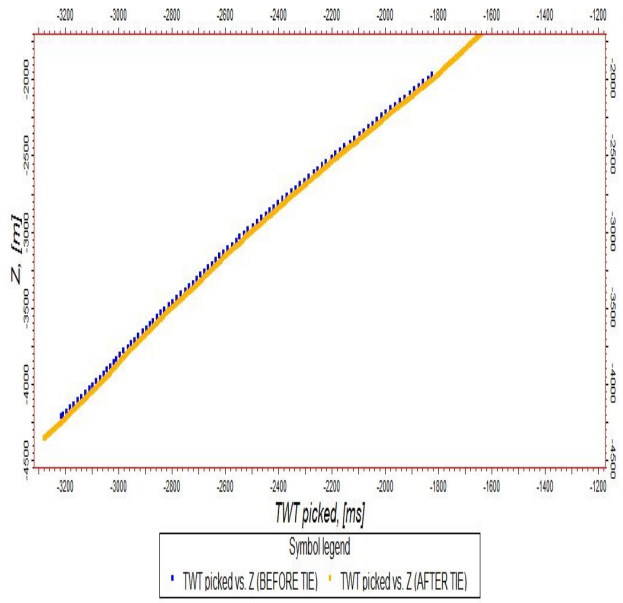

Figure 9: Plot of TDR before and after seismic to well tie

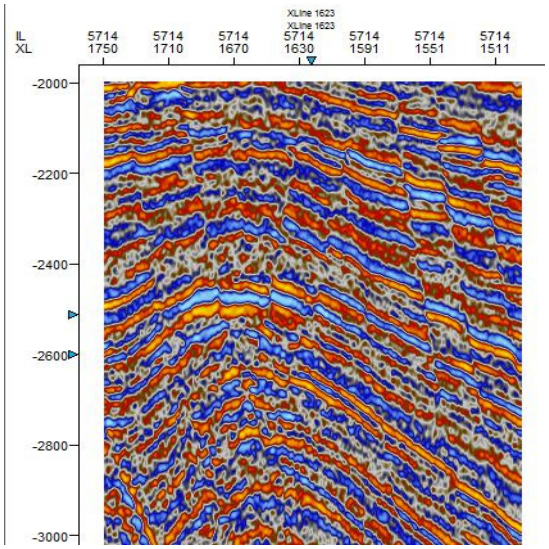

Figure 10: Display of inline 5714 of the original seismic volume

Results of Volume Attributes Realized

Following the extraction of information from the various volume attributes, it was discovered some of the attributes were not appropriate for fault interpretation in Riche field. The original seismic and the realized attributes were compared to discern which can best serve for the faults mapping and the results are displayed on the figures below. The structural smoothing and trace AGC realized on the original Riche seismic volume were suitable but the structural smoothing was preferable for mapping the faults on the inline of the seismic volume on the interpretation window, while the time slice of the variance attribute realized on the structural smoothing attribute made the discontinuities more visible on the 3D window. The structural smoothened (variance) and chaos did not reveal the faults better when compared to the actual Riche seismic and the other volume attributes on the inlines and crosslines.

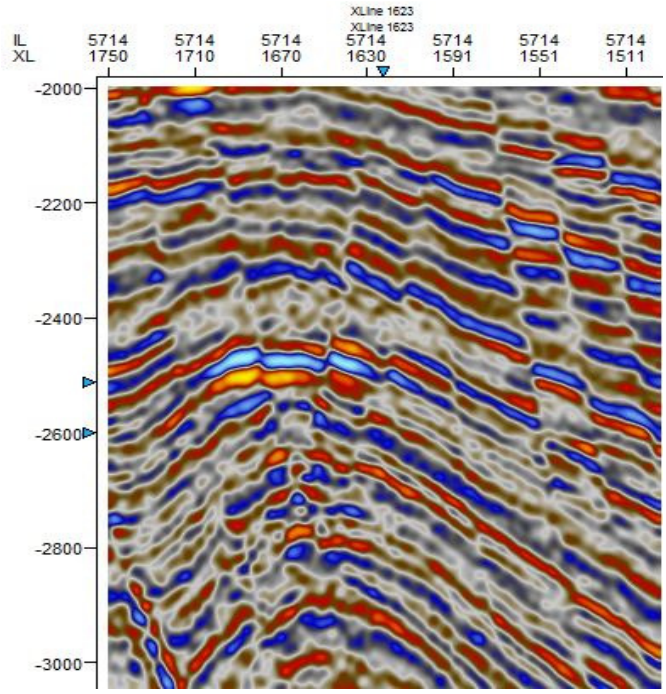

Figure 11: Seismic structural smoothning attribute on inline 5714

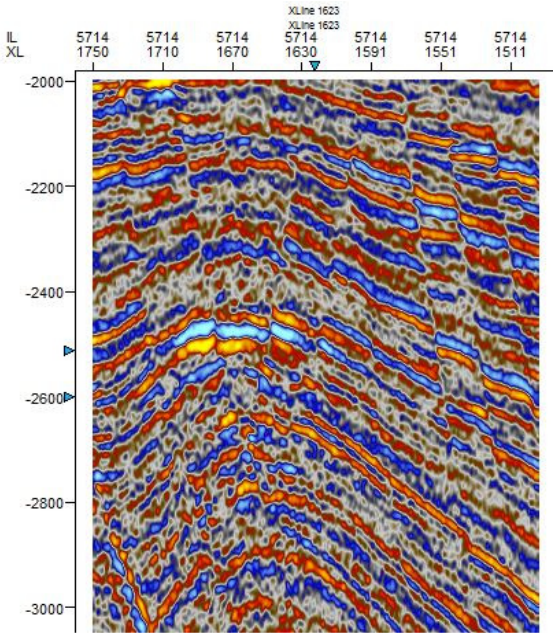

Figure 12: Trace AGC volume attribute on inline 5714

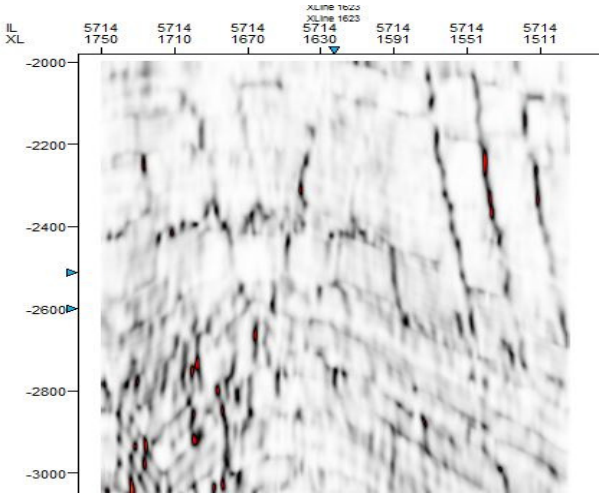

Figure 13: Seismic structural smoothning (variance) attribute on inline 5714

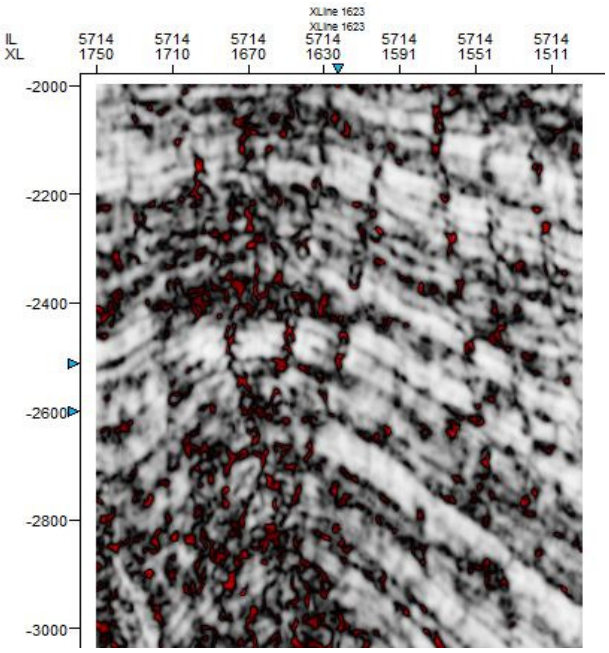

Figure 14: Chaos seismic volume attribute on inline 5714

Faults Interpretation

The Riche field is divided into several major large faults blocks by series of synthetic and antithetic faults mapped on the inline and time slice across the seismic volume as visible in figure 15. The trend of the faults is displayed on the time slice as shown in figure 16.

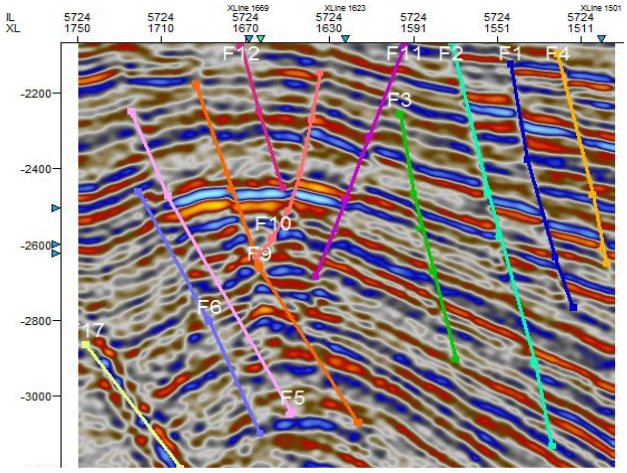

Figure 15: Inline 5724 showing the faults interpreted

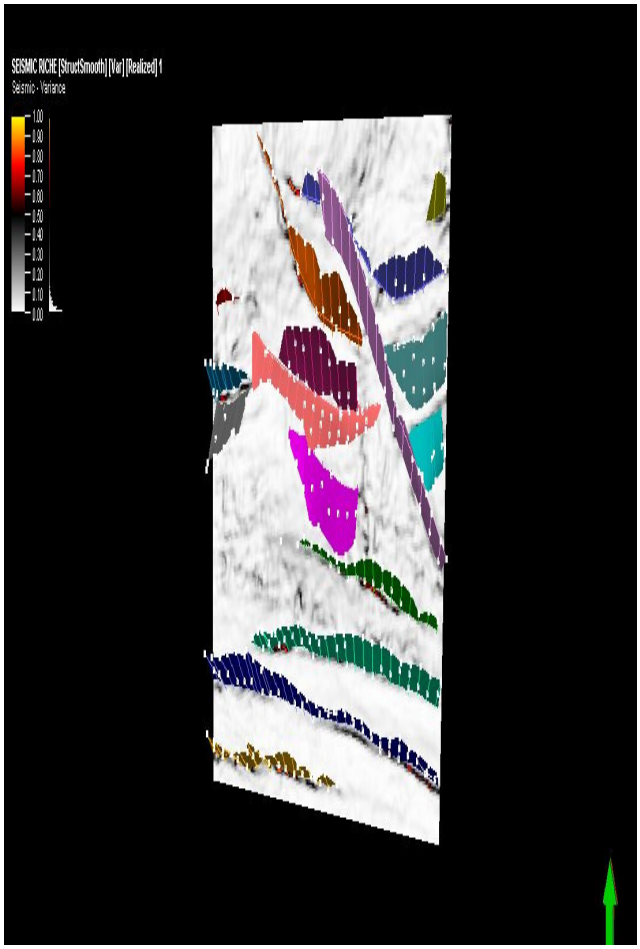

Figure 16: Faults displayed on Structural smoothning variance slice

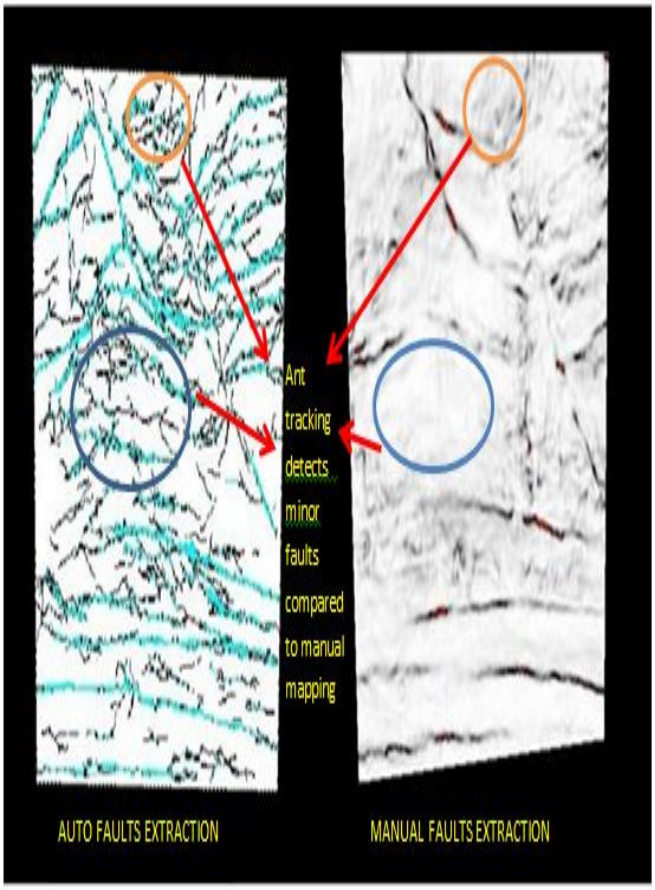

Figure 17: Auto faults slice and manual faults interpretation slice

The ant track automatic faults extracted on different pre-processed volume attributes on time slice 2600s were likened to the manually interpreted faults and it was observed that the ant tracking attribute best reveal even the macro and micro faults that were not ordinarily visible during the manual interpretation. This useful attribute helped to provide a simpler and faster way of picturing the faults trend especially those above the resolution of the seismic data. These micro faults help to deplete resource and cause communication between reservoirs.

Horizon Mapping and Structural Maps Generation

Figure 18 shows the horizon of interest mapped. It is marked with high amplitude and moderate to good continuity. The truncations seen during the mapping was on account of the presence of discontinuous zones. The mapped horizon was then used to produce a seed grid map which was put to use to make a time-domain surface for the Diamond top. The mapped faults and horizon are displayed on figure 19 on the seismic section. The time structural map and eliminated faults polygons generated from the seed grid is revealed in figure 20. The depth converted map shows an accurate structural representation of the horizon.

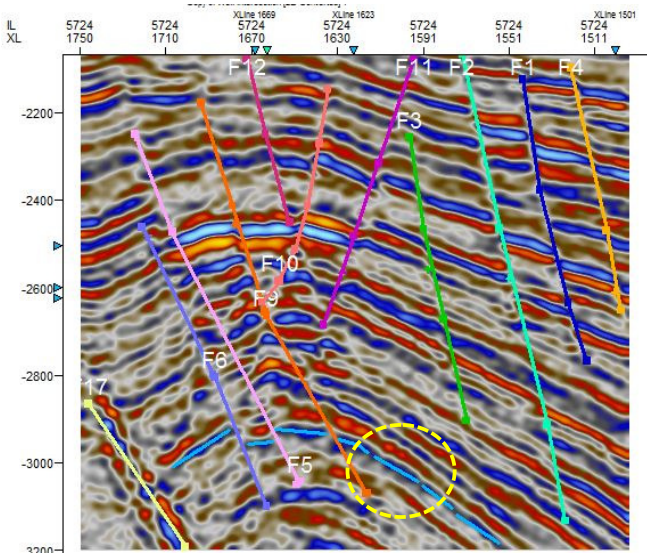

Figure 18: Seismic inline showing horizon picked over the diamond reservoir

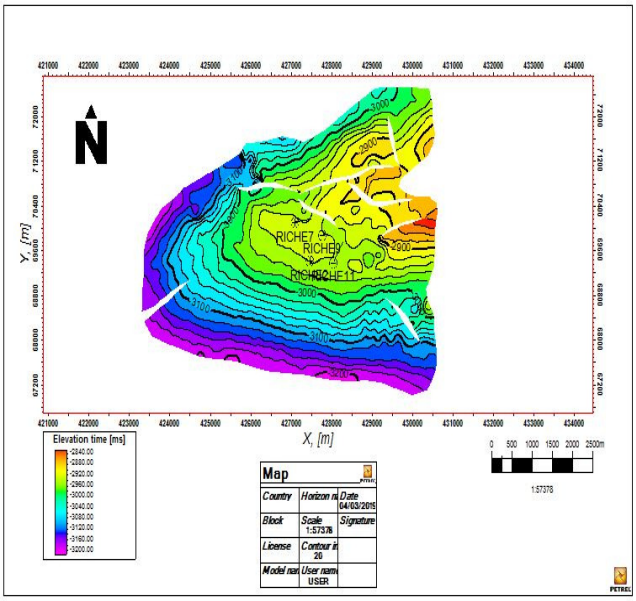

Figure 19: Diamond Horizon Time Structural Map

Observation from the well logs picks shows a sand thinning in the S-E direction. The result from the combination of several volume attribute extractions shows an enhanced 3D volume which aided the subsequent fault identification and manual mapping of the faults.The surface amplitude observations show perfect conformance to structure at the shallower part while amplitude dimming was observed at the deeper part. This dimming could be as a result of energy attenuation caused by the bright amplitude at the shallower part of the cube. The structural expression of the Diamond reservoir sand of gross thickness of 136.44m shows that the faults trend NW-SE direction with an appreciable throw. The Diamond reservoir structure is a 4-way closure accumulation which is impacted by several minor faults at the crestal part with no distinct evidence of major faults. These minor faults may likely not have effect on the dynamic behavior of the field during production.The minor faults partially compartmentalized the Diamond reservoir structure into 4 panels with the available wells (Riche 2, Riche 7, Riche 9 and Riche 11) located on the crestal part of the main structure while the other compartments are potential structure for the further development of the field.

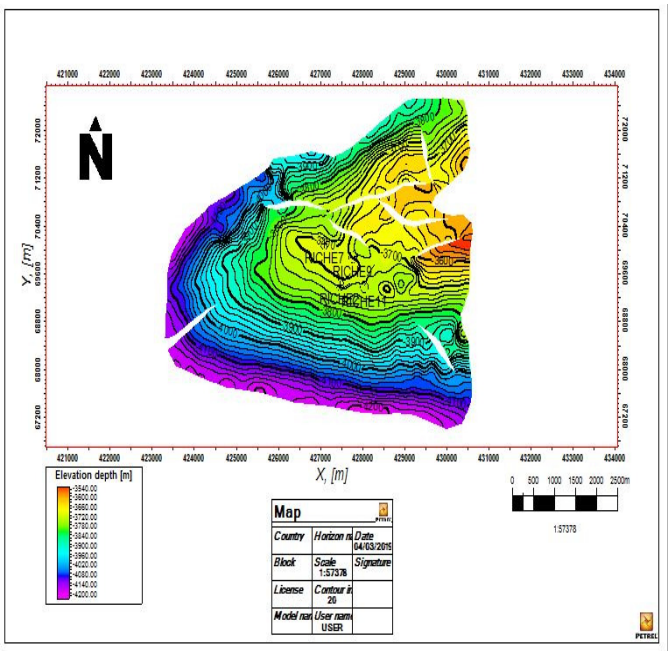

Figure 20: Diamond Horizon Depth Structural Map

IV. DISCUSSION AND CONCLUSION

Summary

The aim and objectives of this research was accomplished using the available seismic and well datasets.A proper reservoir structural characterization was carried out on the Riche Field. Seismic and well log data have thus far applied to clarify structural features of the detected sand bodies within the subsurface of the Riche field. This was achieved by creating time and depth structural contour maps of the horizon interpreted using the Petrel tool. The time-domain and depth-domain structural maps show the structural geometry and potential hydrocarbon trapping system in the subsurface. The anticlinal and fault assisted closures are looked upon as good hydrocarbon prospect zones.

Conclusion

In this research effort, haven carried out a 3-D structural interpretation of the Riche field, characterized structurally by the use of well logs and seismic data sets, the structural maps and seismic section revealed that the principal structure responsible for the hydrocarbon entrapment in the Riche field was the anticlinal structure at the centre of the field which is joined to the crest of the rollover structure and supported by faults.

REFERENCES

[1] Bjørlykke, K. (2010). Petroleum Migration Petroleum Geoscience, Springer Berlin Heidelberg, pp. 349-360.

[2] Christopher Jackson (2012), Seismic Interpretation Lecture Material Department of Earth Science & Engineering, Imperial College.

[3] Henriksen, E., Bjørnseth, H. M., Hals, T. K., Heide, T., Kiryukhina, T., Kløvjan, O. S., Stoupakova, A. (2011), Chapter 17 Uplift and erosion of the greater Barents Sea: impact on prospectivity and petroleum systems. Geological Society, London, Memoirs, 35(1), pp. 270-285.

[4] Lowell,James D . (1985),StructuralStyles i n Petroleum E x p l o r a t i o n , OGCIPublications, p. 458.

[5] Oilfield Review Summary (2011), Basic Petroleum Geochemistry for Source Rock Evaluation.

[6] Robein, E., (2003), Velocities, Time-Imaging, and Depth-Imaging inReflection Seismics: Principles and Methods. EAGE Publications.Houten, Netherlands.

[7] Schlumberger. (2009), Seismic-to-Simulation Software; Seismic Visualization and Interpretation.

[8] Selley, R. C. and Morrill, D. C. (1983), The Reservoir, International Human Resources Development Corporation, U. S.A.

[9] Simm, R. and Bacon, M., (2014), Seismic Amplitude: An Interpreter's Handbook. Cambridge University Press.

[10] Tuttle, M. L. W., R. R. Charpentier and M. E. Brownfield, (1999), The Niger delta petroleum system: Niger delta province, Nigeria, Cameroon, and Equatorial Guinea, Africa: USGS Open-file report.

[11]Zhao, J. and Sun, S.Z., (2013), Automatic fault extraction using a modified ant-colony algorithm: Journal of Geophysics and Engineering, v. 10;pp 1-10.

